Journal of Economics and Administrative Sciences
2024; 30(143), pp. 420-434

P-ISSN 2518-5764
E-ISSN 2227-703X

Journal of Economics and Administrative Sciences (JEAS)

Available online at http://jeasiq.uobaghdad.edu.iq
DOI: https://doi.org/10.33095/59cx4m31

Gaussian Denoising for the First Image from The James Webb Space Telescope "Carina Nebula" using Non-Linear Filters

Mohammed Abdul Wadood *
Department of Statistics
College of Administration and Economics,
University of Baghdad
Iraq, Baghdad
mohamed.a.mohamed@coadec.uobaghdad.edu.iq
https://orcid.org/0000-0003-3267-0546

Asmaa Ghalib Jaber
Department of Statistics
College of Administration and Economics,
University of Baghdad
Iraq, Baghdad
Drasmaa.ghalib@coadec.uobaghdad.edu.iq
https://orcid.org/0000-0002-4988-1924

***Corresponding author**

Received:1/11/2023 Accepted: 18/2/2024 Published Online First: 1 /10/ 2024

This work is licensed under a Creative Commons Attribution-NonCommercial 4.0 International (CC BY-NC 4.0)

Abstract:

Noise, including Gaussian noise, distorts images during transition or acquisition process, reducing required information. Removing or reducing this noise is crucial in image processing. The James Webb Space Telescope (JWST) is a vital tool for enhancing our understanding of the universe, providing valuable scientific data and inspiring global interest. In this paper we introduce several nonlinear (Non-Local Mean, Bilateral, and classical) filters to remove the Gaussian noise from the Carina Nebula Image, the first image taken by (JWST) on 12 July 2022. These nonlinear filters were therefore selected to highlight the significance of selecting the right technique that can handle, process, and preserve as many details as possible. They also serve to elucidate the degree of advancement achieved in the field of denoising and the distinction between the classical filters and the more sophisticated filters that have evolved to handle finer details. Classic filters deal with the pixels themselves and their neighbors and then perform the desired statistical process. While advanced filters consider the similarities and distances between the central pixel and its neighbors, they preserve the edges of the image as advanced features. Based on quality measurements (PSNR) and (SSIM), the filter results were compared. The results show that the Bilateral filter gives high performance in restoring images under different Gaussian noise densities compared with the other denoising filters where it gives values of (30.65) and (0.93) for (PSNR) and (SSIM) respectively Which is higher than the results of the filters.

Paper type :Research paper.

Keywords: Image Denoising; Image Restoration; Gaussian Noise; Non-Local Mean Filter; Bilateral Filter, Classical Filter.

P-ISSN 2518-5764
E-ISSN 2227-703X

1.Introduction:

In many life applications, satellite images are crucial because they provide a precise and unambiguous image of the subject being studied (Abdul Wadood and Ghalib, 2018; Abdul Wadood and Ghalib, 2019). Examples of these applications include tracking the motion of galaxies, planets, and celestial objects and the degree of climate change and rising and falling ocean water levels. According to Muslim and Ghalib (2019) and Ghalib and Abdul Wadood (2020), the satellite image is a digital image that is displayed as a series of numbers that can be saved and managed by a digital computer. The image is split up into tiny sections known as pixels to convert it into numbers (Muslim and Ghalib, 2019). Similar to other types of images, satellite images are subject to noise due to transmission and acquisition (Kolhe and Yogendra, 2013). This might have an impact on image analysis and study. To evaluate and examine the image(s), it is crucial to remove or reduce the noise. According to Swamy and Kulkarn (2020), noise in satellite images is an undesired physical phenomenon that results from variations in atmospheric layers. (Hambal and Faustini, 2017) point out that there are various types of noise, with Gaussian noise being the most prevalent type. Each pixel in the noisy image represents the sum of the true pixel value and a random Gaussian-distributed noise value (Liu and Jianbin, 2018). This statistical noise is known as Additive White Gaussian Noise (AWGN), and it has a probability density function of the normal distribution (Ali, 2018).

In this paper, the problem is the appearance of noise on telescope images during the transmission or acquisition process, which will reduce the quality of the images and thus the quality of analysis and interpretation. The objective is to remove this noise by using nonlinear methods to conserve as much data as possible regarding space telescope images because of their significance for studies and research in science. The nonlocal Mean (NLM) and Bilateral (BF) filters are among the best image-denoising and edge-preserving tasks. (NLM) denoising methods, look for nearby pixels within a sizable search window, and weigh them based on average pixel intensities and similarities (Anh, 2014). These algorithms were developed by Buades et al. (Wilson and Julia, 2013). Whereas (BF) is a straightforward, stable, and noniterative technique, proposed by Manduchi (Manduchi and Tomasi, 2005), reduces noise prevents edges, and considers both spatial and intensity variations from the central pixel (Angulo, 2013). Classic filters are considered the basis or point from which advanced filters started. These filters deal with the image pixels individually, searching for any noise values included in the pixel intensity to remove them.

1.1 Literature Review:

Numerous researchers have attempted to eliminate noise in recent years by using these filters in their studies. These studies provide light on the most notable discoveries in the field of digital image denoising using the filters used in this paper. As a result, we can take advantage of the features and additions made to these techniques to enhance their performance and apply them to our intended research objective. Such as, Ahmood (2015) removed various types of noise added to a grayscale image of size 512 * 512 pixels using both classical and fuzzy filters of size 3*3. The results show that classical methods were able to deal with damaged pixels and gave results close to that of fuzzy filters, despite their superiority. Hossein and Habib (2020) improved SNR quality measurement from 25.1 when using Gaussian filtering to 28.8 when the MRNLM method was used, where this method employed multiple reconstruction NLM filtering (MRNLM) to eliminate redundant information from auxiliary images. Heo et al. (2020) conducted a systematic review to evaluate the efficacy of the NLM denoising algorithm in MR imaging and proved an accurate method for disease diagnosis. Their findings indicate that the NLM denoising algorithm is a viable strategy for accomplishing this objective.

P-ISSN 2518-5764
E-ISSN 2227-703X

Improved methods based on fast or optimization terms and various functions are expected to yield more useful results. Jasim (2020) combined several denoising filters to reduce noise in face images, then, as a preprocessing step, the best of these filters was selected, and PCA was used to perform face recognition. The outcome demonstrated an improved face recognition process under high-density noise by utilizing principal component analysis and the adaptive weighted mean filter. Feng and Pan (2021) proposed a novel algorithm for infrared image enhancement based on the relativity of the Gaussian adaptive bilateral filter that consists of three steps. divide the image by the relativity of the Gaussian-adaptive bilateral filter, multiplied by the proposed weight coefficient, and combine the detail layer and the base layer processed. The suggested algorithm successfully increases the contrast of infrared images, according to the results. Noor (2021) improved ultrasound noisy images in two steps. Stage one involved enhancing the images using 3x3, 5x5, and 7x7 sliding window sizes of adaptive Weiner, Lee, Gamma, and Frost filters; stage two involved simulating the noise in Lina's image using a different percentage of speckle noise. The findings demonstrated that as the slide window size increased, so did the additive noise reduction. Chen and Gao (2022) suggested an NLM algorithm based on the fractional compact finite difference scheme (FCFDS) to reduce speckle noise in OCT images. When compared to integer order difference operators, FCFDS makes greater use of local pixel data. Simulations demonstrate that, in comparison to other cutting-edge despeckling techniques, the suggested method significantly reduces noise and maintains image details. Wagner et al. (2022) suggested a hybrid denoising technique that combines a convolutional deep learning denoising network with a set of trainable joint bilateral filters (JBFs) to predict the guidance image. The outcome demonstrates a high level of noise reduction efficacy. Nabahat et al. (2022) proposed a bilateral filter for image denoising called the whale optimization algorithm (WOA) that depends on appropriate parameter selection. The bilateral filter performance is largely dependent on the proper parameter selection and it is parameters are optimized by using the weighted sum of the (PSNR) and (SSIM) as a fitness function of the WOA algorithm to design the proposed filter. The results show that the recommended approach performs better than the others. Fabian et al. (2022) proposed a bilateral filter that can be integrated into any deep learning algorithm and optimized in a purely data-driven manner by calculating the gradient flow toward its hyperparameters and input. The suggested approach demonstrates the capacity to rival cutting-edge denoising architectures. Abd Almoanf and Shaker (2022) describe a technique based on the retinex algorithm and discrete wavelets transform to improve the quality of computed tomography images by eliminating potential noise. The suggested method aims to improve the contrast of the images. The DCP method with WT was found to have the highest rate of enhancement, according to the experiment results. Xu et al. (2022) proposed a scale adaptive texture filtering algorithm to smooth strong gradient textures while maintaining weak structures. The results demonstrate how well the suggested algorithm performs in removing textures while maintaining main structures and the quality of structure similarity. Spagnolo et al. (2023) developed a novel approximate computing strategy to meet real-time requirements and minimize the computational complexity of the image-denoising process, it is demonstrated that the novel approximate approach can be helpfully exploited in the design of reconfigurable denoising filters able to reach image qualities as close as possible to the precise software counterparts. Liu and Zhang (2023) proposed a novel method of image denoising based on wavelet transform and nonlocal moment mean filtering approach (NMM). The experiments demonstrate that the algorithm achieves a better denoising effect compared with other denoising methods. Huihua et al. (2023) proposed an enhanced NLM denoising algorithm that extracts gradient information from images more precisely by fusing the Laplacian of the Gaussian operator. The suggested algorithm recovers CT images with high PSNR and SSIM values while maintaining the image edge and suppressing noise.

P-ISSN 2518-5764
E-ISSN 2227-703X

The research problem is the appearance of noise on telescope images during the transmission or acquisition process, which will reduce the quality of the images and thus the quality of analysis and interpretation.
The objective is to remove this noise through the use of nonlinear statistical methods, including the proposed method.

2.Material and Methods:

2.1 Non-Local Means Filter (NLM):

The Non-Local Mean Filter (NLM) algorithm was introduced by A. Buades et al. (Wilson and Julia, 2013) and is based on a non-local averaging of all pixels (Dore and Cheriet, 2009; Sarker, 2012). It is a nonlinear filter used to remove Gaussian noise from images while preserving image details (Angella and Rini, 2019). for a pixel (i) in the noise image v = v{v(i) | i∈I}, the estimated value NL[v](i) is calculated as.

$$NL[v] = \sum_{j\epsilon I} w(I,j)v(j) \quad (1)$$

Where w(i, j) is the weights, which satisfy the standard conditions $0 \leq w(i, j) \leq 1$ and $\sum_j w(i, j) = 1$, which are dependent on the similarity between the pixels (i) and (j) (Buades et al, 2005). (N_K) indicates a fixed-size square neighborhood centered at a pixel (k), and the similarity is measured as a decreasing function of the weighted Euclidean distance, and the two pixels (i) and (j) are similar when the intensity of the vectors $v(N_i)$ and $v(N_j)$ are similar.

$$\left\|V(N_i) - v(N_j)\right\|_{2,a}^2 \quad (2)$$

In noisy neighborhoods, the Euclidean distance increases the following equality (Wilson and Julia, 2013).

$$\left\|V(N_i) - v(N_j)\right\|_{2,a}^2 = \left\|v(N_i) - v(N_j)\right\|_{2,a}^2 + 2\sigma^2 \quad (3)$$

Since the order of similarity between pixels is expected to be conserved by the Euclidean distance, it clarifies the robustness of the (NLM) (You, and Nam, 2013). The definition of the weights is:

$$w(i,j) = \frac{1}{Z(i)} e^{\frac{-\left\|v(N_i)-v(N_j)\right\|_{2,a}^2}{h^2}} \quad (4)$$

where Z(i) is the normalizing constant and (h) is the filtering degree or smoothing parameter.

$$Z(i) = \sum e^{\frac{-\left\|v(N_i)-v(N_j)\right\|_{2,a}^2}{h^2}} \quad (5)$$

It regulates the weights' decay as a function of Euclidean distances by controlling the exponential function's decay. This image filter's implementation method is explained by the algorithm that follows.

P-ISSN 2518-5764
E-ISSN 2227-703X

Step 1: Input the color image "Carina Nebula".
Step 2: Add Gaussian noise to the input image with a mean and sigma to obtain a noisy image.
Step 2: Convert the noisy image from RGB color space to YUV color space to obtain a YUV image.
Step 3: Extract the luminance channel Y from the YUV image.
Step 4: Apply NLM filtering to the luminance channel Y by calculate the similarity to obtain a filtered luminance channel FY.
Step 5: Replace the original luminance channel Y with the filtered luminance channel FY.
Step 6: Convert the filtered YUV back to RGB color space to obtain the denoised color image.
Step 7: Output the denoised color image.

2.2 Bilateral Filter (BF):

A bilateral filter is a nonlinear filter used for edge preservation and image smoothing (Anchal et al., 2018; Liu et al., 2020). It measures proximity in intensity space using a separate kernel, in contrast to traditional convolutional filters (Ghosh et al., 2018). (BF) is defined as a weighted average of adjacent pixels (Chen et al., 2020):

$$\mathrm{BF}[\mathrm{I}]_{\mathrm{p}} = \frac{1}{\mathrm{W_p}} \sum_{\mathrm{q}\in \mathrm{s}} \mathrm{G}_{\sigma_\mathrm{s}}(\|\mathrm{p}-\mathrm{q}\|)\mathrm{G}_{\sigma_\mathrm{r}}(\|\mathrm{I_p}-\mathrm{I_q}\|)\mathrm{I_q} \qquad (6)$$

where (Wp) is the normalization factor, which is defined as follows (Kaur and Bhawna, 2020):

$$\mathrm{W_p} = \sum_{\mathrm{q}\in \mathrm{s}} \mathrm{G}_{\sigma_\mathrm{s}}(\|\mathrm{p}-\mathrm{q}\|)\mathrm{G}_{\sigma_\mathrm{r}}(\|\mathrm{I_p}-\mathrm{I_q}\|)\mathrm{I_q} \qquad (7)$$

The parameter σ_s and σ_r will determine the degree of filtering applied to the image (I). When the intensity values of (q) pixels differ from (Ip), the Gaussian range (G_{σ_r}) reduces the influence of (q) pixels. (G_{σ_s}) is a Gaussian weight that decreases the influence of distant pixels. This image filter's implementation method is explained by the algorithm that follows.

Step 1: Input the color image "Carina Nebula".
Step 2: Add Gaussian noise to the input image with a mean and sigma to obtain a noisy image.
Step 2: Convert the noisy image from RGB color space to YUV color space to obtain a YUV image.
Step 3: Extract the luminance channel Y from the YUV image.
Step 4: Apply bilateral filtering to the luminance channel Y by measuring proximity in intensity to obtain a filtered luminance channel FY.
Step 5: Replace the original luminance channel Y with the filtered luminance channel FY.
Step 6: Convert the filtered YUV back to RGB color space to obtain the denoised color image.
Step 7: Output the denoised color image.

2.3 Classical Filters:

Classical filters deal with pixel values or pixel neighbors of the noisy image (Stella and Bhushan, 2012). Numerous filters fall into the category of classical filters, including non-linear filters like midpoint filter (Mid), median filter (Med), minimum value filter (Min), and maximum value filter (MAX). This filter is widely used and is regarded as the foundation for all other filters. The (Med) filter, which is defined by the following equation (Dubeya, 2022), substitutes the median of the neighborhood intensities for the pixel value in the new image (Rajni and Anutam, 2014).

$$\hat{\mathrm{f}}(\mathrm{x},\mathrm{y}) = \mathrm{median}_{(\mathrm{s},\mathrm{t})\in \mathrm{S_{xy}}}\{\mathrm{g}(\mathrm{s},\mathrm{t})\} \qquad (8)$$

P-ISSN 2518-5764
E-ISSN 2227-703X

Where (x, y), (s, t) are pixel coordinates of the estimated and noisy images f(x,y), g(s,t) respectively. Assuming we have a (3×3) image, we can apply a (3×3) mask of the (Med) filter to it as Figure 1 below illustrates:

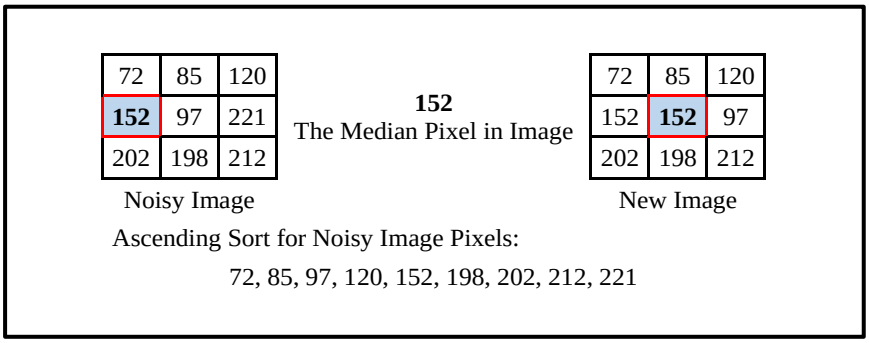

Figure 1: Median Filter

Next, the (Med) filter effectively sorts the image's pixels in ascending order based on their intensities. After that, it chooses the median pixel value and substitutes it for the center pixel's value in the newly created (non-noisy) image (Ullah, 2018). The median denotes the (50^{th}) percentile of a ranked set of numbers (Pathidar, 2010). In contrast, the (Max) filter is represented by the (100th) percentile, as stated by (Kommineni and Hemantha, 2019):

$$\hat{F}(x,y) = \max_{(s,t)\in S_{xy}}\{g(s,t)\} \quad (9)$$

Where (x, y), (s, t) are pixel coordinates of the estimated and noisy images f(x,y), g(s,t) respectively. This filter seeks to Find the brightest pixel in the image (Kumar, 2014), Figure 2 illustrates the Max filter.

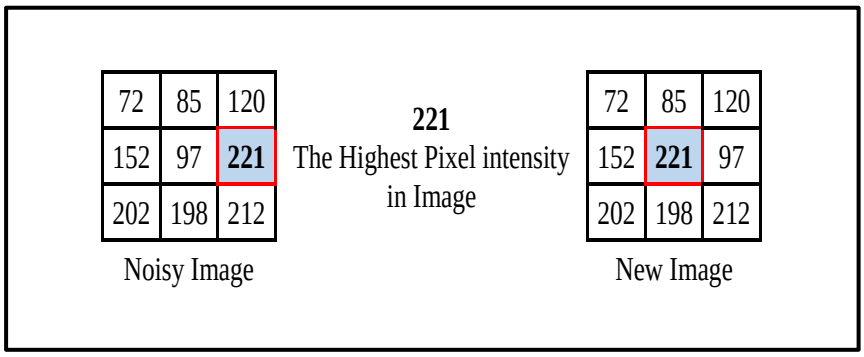

Figure 2: Maximum Value Filter

Conversely, the (Min) filter represents the (0^{th}) percentile filter and is provided by:

$$\hat{F}(x,y) = \min_{(s,t)\in S_{xy}}\{g(s,t)\} \quad (10)$$

Where (x, y), (s, t) are pixel coordinates of the estimated and noisy images f(x,y), g(s,t) respectively. This filter is used to identify the darkest areas of an image (Singh and Nirvair, 2014). An example of this filter is shown in Figure 3.

P-ISSN 2518-5764
E-ISSN 2227-703X

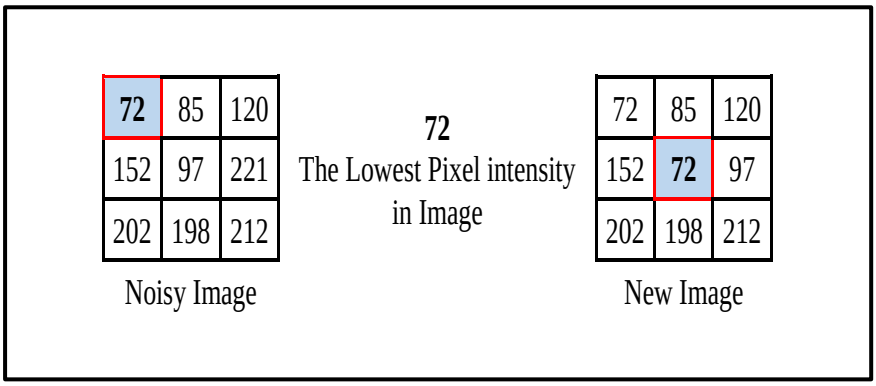

Figure 3: Minimum Value Filter

The midpoint filter is the arithmetic mean of the MAX and MIN value filters that are calculated by the equation (Singh and Nirvair, 2014).

$$\hat{f}(x,y) = \frac{1}{2}\left[\max_{(s,t)\in S_{xy}}\{g(s,t)\} + \min_{(s,t)\in S_{xy}}\{g(s,t)\}\right] \quad (11)$$

It combines averaging and order statistics as shown in Figure 4.

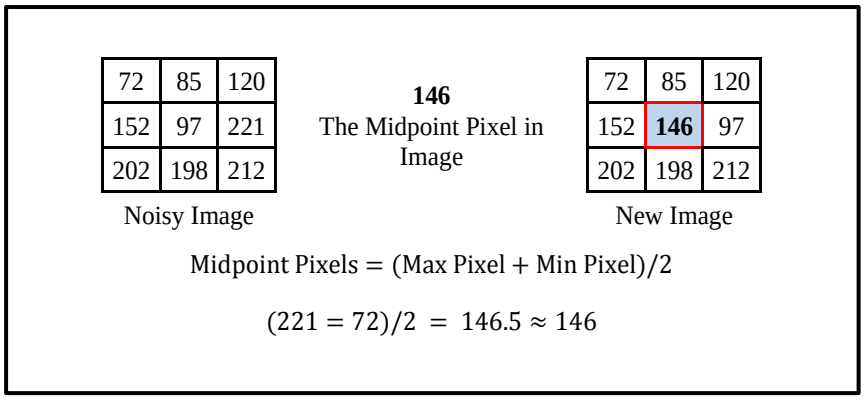

Figure 4: Midpoint Value Filter

3. Discussion of Results:

The experiment was carried out by adding AWGN with zero mean and 0.01 variance to the approved image as shown in Figure 5, which is the first James Webb space telescope image taken to the Carina Nebula on July 12, 2022 (https://webb.nasa.gov/). With thousands of astronomers using JWST worldwide, JWST is the leading observatory of the coming ten years. It takes images from the first bright lights following the Big Bang to the creation of solar systems that could support life on planets like Earth and the development of our own Solar System, it examines every stage of our Universe's history. So, this image must be clear and free of impurities .Considering the significance of these images, we should work to eliminate any noise that may have been introduced during the transmission and acquisition process. So, in this experiment, we added different percentages of Gaussian noise to the adopted image and then applied the adopted filters, the code of these filters is written using MATLAB.

P-ISSN 2518-5764
E-ISSN 2227-703X

A

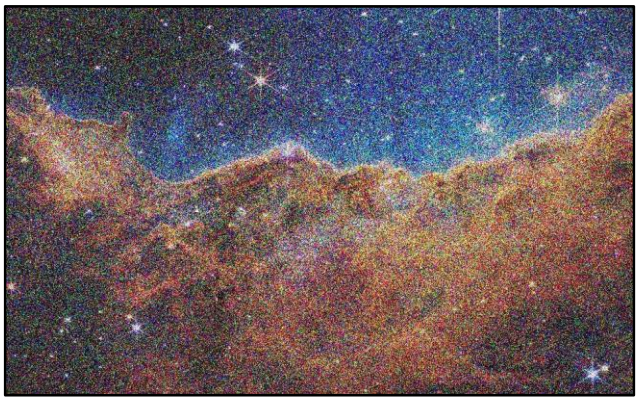

B

Figure 5: Original Image of Carina Nebula (**A**), Gaussian Noise Image of Carina Nebula (**B**).

To evaluate the quality of the obtained results the Structural Similarity Index Measure (SSIM) and the Peak Signal to Noise Ratio (PSNR) are used to calculate this quality. Where (PSNR) is regarded as a quality measurement that is frequently used to quantify reconstruction quality for images and video (Hore and Djemel, 2010):

$$\mathrm{PSNR} = 10 * \log_{10} * \left(\frac{255^2}{\mathrm{MSE}_{(x,y)}}\right) \quad (12)$$

Where:

$$\mathrm{MSE}_{(x,y)} = \frac{1}{MN}\sum_{i=1}^{M}\sum_{j=1}^{n}(x_{ij} - y_{ij})^2 \quad (13)$$

On the other hand, (SSIM) is a quality measure that determines how similar the two digital image structures are (Wang et al., 2004). The following equation provides it:

$$\mathrm{SSIM} = (l(x,y))^{\alpha} * \left(c(x,y)\right)^{\beta} * (s(x,y))^{\gamma} \quad (14)$$

P-ISSN 2518-5764
E-ISSN 2227-703X

Which stand for three weights (Bakurov et al., 2022) with exponents (α), (β), and (γ), respectively.

$$I(x,y) = \frac{2\mu_x\mu_y + C_1}{\mu_x^2 + \mu_y^2 + C_1} \quad (15)$$

$$C(x,y) = \frac{2\sigma_x\sigma_y + C_2}{\sigma_x^2 + \sigma_y^2 + C_2} \quad (16)$$

$$S(x,y) = \frac{\sigma_{xy} + C_3}{\sigma_x\sigma_y + C_3} \quad (17)$$

Where C1, C2, and C3 are small quantities for numerical stability. To assess the efficacy of the approved filters, we added different amounts of Gaussian noise ratios to the image. Where The quality of the restored images varies, as Table 1 illustrates. The results indicate that the Bilateral filter performs best in terms of both PSNR and SSIM when there is a noise density of 0.01 where it is given the values 30.65 PSNR, and 0.93 SSIM respectively, while the Nonlocal mean filters rank second with 24.32 PSNR and 0.89 SSIM. According to measurements, the median filter from the classical filters has the highest quality measures 22.84 PSNR and 0.87 SSIM, respectively. The Midpoint filter comes in the second rank with measurements of 22.27 PSNR and 0.86 SSIM. In contrast, the results of the minimum and maximum value filters are 16.32 PSNR, 0.77 SSIM, and 17.66 PSNR, 0.74 SSIM respectively. Figure 6 displays the images that have been restored.

Table 1: PSNR and SSIM values for the restored images of each filter

Filters	Image Quality Measurements	
	PSNR	SSIM
Bilateral	30.65	0.93
NLM	24.32	0.89
Maximum Value	16.32	0.77
Minimum Value	17.66	0.74
Median Value	22.84	0.87
Midpoint Value	22.27	0.86

The following outcomes are obtained when we apply the filters to denoise the Carina Nebula image at different noise ratios of 50%, and 75%:

Table 2: PSNR and SSIM values of the restored images calculated for different noise ratio

Filters	Image Quality Measurements in Different Noise Ratios			
	50%		75%	
	PSNR	SSIM	PSNR	SSIM
Bilateral	34.63	0.99	34.95	0.99
NLM	13.12	0.80	12.63	0.80
Maximum Value	7.35	0.56	7.07	0.55
Minimum Value	9	0.52	8.59	0.5
Median Value	12.66	0.78	12.17	0.78
Midpoint Value	12.43	0.77	12.01	0.77

P-ISSN 2518-5764
E-ISSN 2227-703X

Figure 6: Restored Images of Carina Nebula by, Bilateral Filter (**A**), Nonlocal Mean Filter (**B**), Max Filter (**C**), Min Filter (**D**), Median Filter (**E**), and Midpoint Filter (**F**).

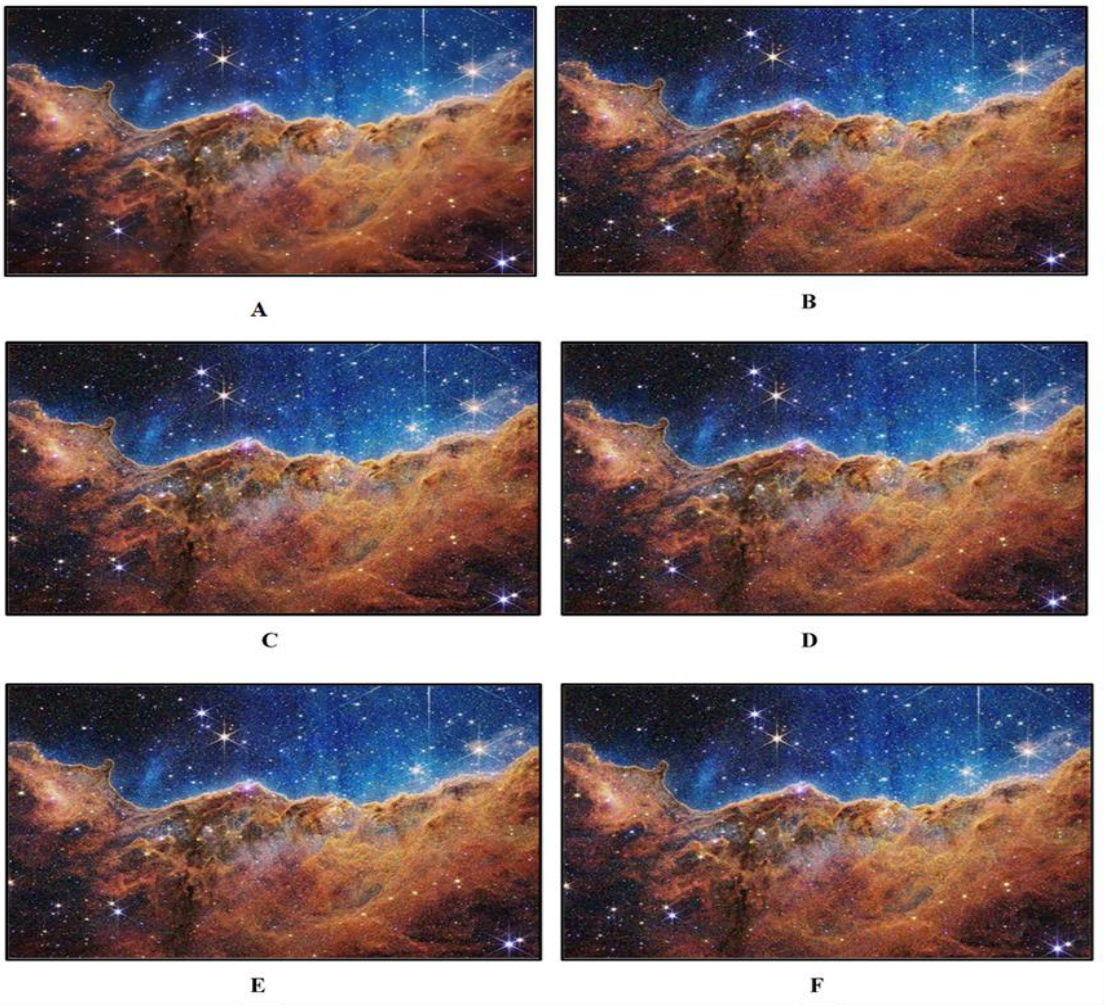

We can observe from the results in Table 2 that the order of filters about the restored image quality and the presence of various noise levels did not change. The first filter is bilateral, which has 34.63 PSNR and 0.99 SSIM in 50% and 34.95 PSNR and 0.99 SSIM in 75% noise density, respectively. The maximum value filter is at the bottom of the ranking, as recorded 7.35 PSNR, 0.65 SSIM in 50% noise density, and 7.07 PSNR, 0.55 SSIM in 75% noise density. the second one is the NLM filter with 13.12 PSNR, 0.80 SSIM in 50% noise density, 12.63 PSNR, and 0.80 SSIM in 75% noise density.

The advantage of the bilateral filter is reducing noise while preserving edges in the image because it gives higher weight to pixels that are both spatially close and have similar intensity values. This way, noise is suppressed, and edges are preserved, making the filtered image visually smoother while retaining important features. On the other hand, the nonlocal mean filter is a versatile and effective denoising technique that considers the global structure of an image. but it a computationally intensive, and needs optimizations and variations to make it more practical for real-world applications.

P-ISSN 2518-5764
E-ISSN 2227-703X

4. Conclusion:

The results show that the bilateral filter was quite flexible in reducing noise while maintaining all the qualities and features of the original image. It achieved a high image quality index and moved the PSNR away from its nearest filter by almost ten degrees. Furthermore, the Bilateral filter stands out for maintaining image contrast and edges, as evidenced by the structural similarity quality index (SSIM), which awarded the filter a high-efficiency level of 0.93. This is not to say that the other filters are not effective; in fact, classic filters are based on local information and are simple to compute but may not preserve fine details well. They are thought of as the initial stage towards creating effective filters that address the features or attributes of the noise, which is reflected in the caliber of the denoised images. On the other hand, the nonlocal mean filter considers the global structure of the image, providing better preservation of edges and details, but at a higher computational cost, it is regarded as one of the most cutting-edge and effective filters for noise reduction, as demonstrated by its performance. Ultimately, the findings demonstrate that the quality of the restored image decreases with increasing added noise density.

5. Acknowledgments:

The image of the Carina Nebula, the furthest point in the universe that humans can reach, is one of the images from the James Webb space telescope (JWST) that the author is grateful for being provided by the US National Aeronautics and Space Administration Agency (NASA) https://webb.nasa.gov/.

Authors Declaration:

Conflicts of Interest: None

-We Hereby Confirm That All The Figures and Tables In The Manuscript Are Mine and Ours. Besides, The Figures and Images, Which are Not Mine, Have Been Permitted Republication and Attached to The Manuscript.

- Ethical Clearance: The Research Was Approved By The Local Ethical Committee in The University.

References:

1. Abd Almoanf, D. and Shaimaa, H. 2022. Medical Image Enhancement Techniques. *Iraqi Journal of Computer Communication Control and System Engineering*, 22(4), pp.48–59. https://doi:10.33103/uot.ijccce.22.4.5.

2. Abdul Wadood, M. and Ghalib, A. 2019. Split and Merge Regions of Satellite Images Using the Non-Hierarchical Algorithm of Cluster Analysis. *Journal Of Economics and Administrative Sciences*, 25(111), pp.466–484. https://doi.org/https://doi.org/10.33095/jeas.v25i111.1638.

3. Abdul Wadood, M. and Ghalib, A. 2018. Use Some Statistical Algorithms in Mock Hacking Satellite Images. *Journal Of Economics and Administrative Sciences*, 108(24), pp.474–487.

4. Ahmood, T. 2015. Comparative Study between Classical and Fuzzy Filters for Removing Different Types of Noise from Digital Images. *Iraqi Journal of Science*, 56(1), pp.558–576.

5. Ali, M. 2018. MRI Medical Image Denoising by Fundamental Filters. *High-Resolution Neuroimaging - Basic Physical Principles and Clinical Applications*, 43(17), pp.658–666. https://doi.org/10.5772/intechopen.72427.

6. Anchal, A., Sumit, B., Bhawna, G., Ayush, D. and Sunil, A. 2018. An Efficient Image Denoising Scheme for Higher Noise Levels Using Spatial Domain Filters. *Biomedical and Pharmacology Journal*, 11(2), pp.625–634. https://doi.org/10.13005/bpj/1415.

7. Angella, S., Ari, S. and Rini, I. 2019. Application of Denoising Non-Local Mean Filter (NLM) in MRI Brain Image T2WI TSE SENSE. *International Journal of Allied Medical Sciences and Clinical Research (IJAMSCR)*, 7(3), pp.1033–1039.

8. Angulo, J. 2013. Morphological Bilateral Filtering. *SIAM Journal on Imaging Sciences*, 6(3), pp.1790–1822. https://doi:10.1137/110844258.
9. Anh, N. 2014. Image Denoising by Adaptive Non-Local Bilateral Filter. *International Journal of Computer Applications*, 99(12).
10. Arabi, H, and Habib Z. 2020. Non-Local Mean Denoising Using Multiple Pet Reconstructions. *Annals of Nuclear Medicine*, 35(2), pp.176–186. https://doi.org/10.1007/s12149-020-01550-y.
11. Bakurov, I., Marco, B., Raimondo, S., Mauro, C. and Leonardo, V. 2022. Structural Similarity Index (SSIM) Revisited: A Data-Driven Approach. *Expert Systems with Applications*, 25(189). https://doi.org/10.1016/j.eswa.2021.116087.
12. Buades, A., B. Coll, and Morel, M. 2005. A Non-Local Algorithm for Image Denoising. *IEEE Computer Society Conference on Computer Vision and Pattern Recognition (CVPR'05)*, 2(16). https://doi.org/10.1109/cvpr.2005.38.
13. Chen, B., Yi-Syuan, T. and Jia-Li, Y. 2020. Gaussian-Adaptive Bilateral Filter. *IEEE Signal Processing Letters*, 15(27), pp.1670–1674. https://doi.org/10.1109/lsp.2020.3024990.
14. Chen, H. and Jing, G. 2022. Non-Local Mean Denoising Algorithm Based on Fractional Compact Finite Difference Scheme Effectively Reduces Speckle Noise in Optical Coherence Tomography Images. *Micromachines*, 13(12), pp.2039-2039. https://doi.org/10.3390/mi13122039.
15. Dore, V. and Cheriet, M. 2009. Robust NL-Means Filter with Optimal Pixel-Wise Smoothing Parameter for Statistical Image Denoising. *IEEE Transactions on Signal Processing*, 57(5), pp.1703–1716. https://doi:10.1109/tsp.2008.2011832.
16. Dubeya, P. 2022. Comparative Performance Analysis of Spatial Domain Filtering Techniques in Digital Image Processing for Removing Different Types of Noise. *International Journal of Nonlinear Analysis and Applications*, 25(13), pp.117–125.
17. Feng, X. and Zhongliang, P. 2021. Detail Enhancement for Infrared Images Based on Relativity of Gaussian-Adaptive Bilateral Filter. *OSA Continuum*, 4(10), pp.2671-2676. https://doi.org/10.1364/osac.434858.
18. Ghalib, A. and Abdul Wadood, M. 2020. Using Multidimensional Scaling Technique in Image Dimension Reduction for Satellite Image. *Periodicals of Engineering and Natural Sciences*, 8(1), pp.447–454. http://dx.doi.org/10.21533/pen.v8i1.1171.
19. Ghosh, S., Pravin, N. and Kunal, C. 2018. Optimized Fourier Bilateral Filtering. *IEEE Signal Processing Letters*, 25(10), pp.1555–1559. https://doi.org/10.1109/lsp.2018.2866949.
20. Hambal, A., Zhijun, P. and Faustini, I. 2017. Image Noise Reduction and Filtering Techniques. *International Journal of Science and Research (IJSR)*, 6(3), pp.2033–2038. https://doi.org/ 10.21275/25031706.
21. Heo, Y., Kyuseok, K. and Youngjin, L. 2020. Image Denoising Using Non-Local Means (NLM) Approach in Magnetic Resonance (MR) Imaging: A Systematic Review. *Applied Sciences*, 10(20), pp.7028-7028. https://doi.org/10.3390/app10207028.
22. Hore, A. and Djemel, Z. 2010. Image Quality Metrics: PSNR vs. SSIM. *2010 20th International Conference on Pattern Recognition*. 12(22). https://doi.org/10.1109/icpr.2010.579.
23. Huihua, K., Gao, W. and Di, Y. 2023. An Improved Non-Local Means Algorithm for CT Image Denoising, 82(5). https://doi.org/10.21203/rs.3.rs-2915903/v1.
24. Jasim, N. 2020. Performance Enhancement of Face Recognition under High-Density Noise Using PCA and de-Noising Technique. *Ibn AL- Haitham Journal for Pure and Applied Sciences*, 33(4), pp.148-154, https://doi:10.30526/33.4.2527.
25. Kaur, B., Ayush, D. and Bhawna G. 2020. Comparative Analysis of Bilateral Filter and Its Variants for Magnetic Resonance Imaging. *The Open Neuroimaging Journal*, 13(1), pp.21–29. https://doi.org/10.2174/1874440002013010021.

26. Kolhe, Y. and Yogendra, J. 2013. Removal of Salt and Pepper Noise from Satellite Images. *International Journal of Engineering Research and Technology (IJERT)*, 2(11), pp.2051–2058. https://doi.org/10.17577/IJERTV2IS110634.
27. Kommineni, V. and Hemantha, K. 2019. Image Denoising Techniques. *International Journal of Recent Technology and Engineering (IJRTE)*, 7(5), pp. 417–419.
28. Kumar, P. 2014. Image Filtering Using Linear and Non-Linear Filter for Gaussian Noise. *International Journal of Computer Applications*, 93(8), pp. 29–34, https://doi:10.5120/16237-5760.
29. Liu, B. and Jianbin, L. 2018. Non-Local Mean Filtering Algorithm Based on Deep Learning. *MATEC Web of Conferences*, 23(2). https://doi.org/10.1051/matecconf/201823203025.
30. Liu, C. and Li, Z. 2023. A Novel Denoising Algorithm Based on Wavelet and Non-Local Moment Mean Filtering. *Electronics*, 12(6). https://doi.org/10.3390/electronics12061461.
31. Liu, W., Pingping, Z., Xiaogang, C., Chunhua, S., Xiaolin, H. and Jie, Y. 2020. Embedding Bilateral Filter in Least Squares for Efficient Edge-Preserving Image Smoothing. *IEEE Transactions on Circuits and Systems for Video Technology*, 30(1), pp.23–35. https://doi.org/10.1109/tcsvt.2018.2890202.
32. Muslim, A. and Ghalib, A. 2019. Comparison Between the Method of Principal Component Analysis and Principal Component Analysis Kernel for Imaging Dimensionality Reduction. *Journal Of Economics and Administrative Sciences*, 16(2), pp.11–24. https://doi.org/https://doi.org/10.33899/iqjoss.2019.164189.
33. Muslim, A. and Ghalib, A. 2019. Use Principal Component Analysis Technique to Dimensionality Reduction to Multi-Source. *Journal Of Economics and Administrative Sciences*, 25(115), pp.464–473. https://doi.org/https://doi.org/10.33095/jeas.v25i115.1778.
34. Nabahat, M., Farzin, K. and Nima, N. 2022. Optimization of Bilateral Filter Parameters Using a Whale Optimization Algorithm. *Research in Mathematics*, 9(1). https://doi.org/10.1080/27684830.2022.2140863.
35. Patidar, P. 2010. Image De-Noising by Various Filters for Different Noise. *International Journal of Computer Applications*, 9(4), pp.45–50 https://doi:10.5120/1370-1846.
36. Rajni and Anutam. 2014. Image Denoising Techniques Overview. *International Journal of Computer Applications*, 86(16), pp.13–17. https://doi:10.5120/15069-3436.
37. Resham, H. 2021. Noise Reduction, Enhancement, and Classification for Sonar Images. *Iraqi Journal of Science*, 39(8), pp.4439–4452, https://doi:10.24996/ijs.2021.62.11(si).25.
38. Sarker, S. 2012. Use of Non-Local Means Filter to Denoise Image Corrupted by Salt and Pepper Noise. *Signal and amp Image Processing: An International Journal*, 3(2), pp.223–235. https://doi.org/10.5121/sipij.2012.3217.
39. Singh, I. and Nirvair, N. 2014. Performance Comparison of Various Image Denoising Filters under Spatial Domain. *International Journal of Computer Applications*, 96(19), pp.21–30. https://doi:10.5120/16903-6969.
40. Spagnolo, F., Pasquale, C., Fabio, F. and Stefania, P. 2023. Design of Approximate Bilateral Filters for Image Denoising on FPGAS. *IEEE Access*, 9(11), pp.1990–2000. https://doi.org/10.1109/access.2022.3233921.
41. Stella, A. and Bhushan, T. 2012. Implementation of Order Statistic Filters on Digital Image and OCT Image: A Comparative Study. *International Journal of Modern Engineering Research (IJMER)*, 2(5), pp.3143–3145.
42. Swamy, S. and Kulkarn, P. 2020. A Basic Overview of Image Denoising Techniques. *International Research Journal of Engineering and Technology (IRJET)*, 7(5), pp.850–857.
43. Tomasi, C. and Manduchi, R. 2005. Bilateral Filtering for Gray and Color Images. *Sixth International Conference on Computer Vision (IEEE Cat. No.98CH36271)*. 22(16). https://doi.org/10.1109/iccv.1998.710815.

44. Ullah, F. 2018. An Efficient Algorithm for Image De-Noising by Using Adaptive Modified Decision-Based Median Filters. *ICST Transactions on Scalable Information Systems*, 10(36), pp.163-173. https://doi:10.4108/eai.27-1-2022.173163.
45. Wagner, F., Mareike, T., Felix, D., Mingxuan, G., Mayank, P., Stefan, P., Noah, M., Laura, P., Yixing, H. and Andreas, M. 2022. Trainable Joint Bilateral Filters for Enhanced Prediction Stability in Low-Dose CT. *Scientific Reports*, 12(1). https://doi.org/10.1038/s41598-022-22530-4.
46. Wagner, F., Mareike, T., Mingxuan, G., Yixing, H., Sabrina, P., Mayank, P. and Stefan, P. 2022. Ultralow-parameter Denoising: Trainable Bilateral Filter Layers in Computed Tomography. *Medical Physics*, 49(8), pp.5107–5120. https://doi.org/10.1002/mp.15718.
47. Wang, Z., Bovik, C. Sheikh, R. and Simoncelli, P. 2004. Image Quality Assessment: From Error Visibility to Structural Similarity. *IEEE Transactions on Image Processing*, 13(4), pp.600–612. https://doi.org/10.1109/tip.2003.819861.
48. Wilson, B. and Julia, D. 2013. A Survey of Non-Local Means Based Filters for Image Denoising. *International Journal of Engineering Research and Technology (IJERT)*, 2(10), pp.3768–3771.
49. Xu, H., Zhongrong, Z., Yin, G., Haizhong, L., Feng, X. and Jun, L. 2022. Adaptive Bilateral Texture Filter for Image Smoothing. *Frontiers in Neurorobotics*, 48(16). https://doi.org/10.3389/fnbot.2022.729924.
50. You, J. and Nam, C. 2013. An Adaptive Bandwidth Nonlocal Means Image Denoising in Wavelet Domain. *EURASIP Journal on Image and Video Processing*, 20(1). https://doi.org/10.1186/1687-5281-2013-60.

Journal of Economics and Administrative Sciences
2024; 30(143), pp. 420-434

P-ISSN 2518-5764
E-ISSN 2227-703X

تقليل الضوضاء الغاوسية لصورة "سديم كارينا" اول صورة ملتقطة من تلسكوب جيمس ويب الفضائي باستخدام المرشحات غير الخطية

محمد عبد الودود محمد[1]
جامعة بغداد/ كلية الإدارة والاقتصاد/ قسم الإحصاء
العراق، بغداد
mohamed.a.mohamed@coadec.uobaghdad.edu.iq
https://orcid.org/0000-0003-3267-0546

أسماء غالب جابر[2]
جامعة بغداد/ كلية الإدارة والاقتصاد/ قسم الإحصاء
العراق، بغداد
Drasmaa.ghalib@coadec.uobaghdad.edu.iq
https://orcid.org/0000-0002-4988-1924

Received:1/11/2023 Accepted: 18/2/2024 Published Online First: 1 /10/ 2024

هذا العمل مرخص تحت اتفاقية المشاع الابداعي نسب المُصنَّف - غير تجاري - الترخيص العمومي الدولي 4.0
Attribution-NonCommercial 4.0 International (CC BY-NC 4.0)

مستخلص البحث:
الضوضاء، بما في ذلك الضوضاء الغاوسية، تؤدي الى تشويه الصور أثناء عملية النقل أو الاستحواذ، مما يقلل من المعلومات المطلوبة، وتعد عملية إزالة هذا التشويش أو تقليله أمراً بالغ الأهمية في معالجة الصور، في حين يلعب تلسكوب الفضاء جيمس ويب (JWST) دوراً حيوياً لتعزيز فهمنا للكون، وتوفير بيانات علمية قيمة، وإلهام الاهتمام العالمي. في هذا البحث قدمنا العديد من المرشحات غير الخطية (المتوسطة غير المحلية والثنائية والكلاسيكية) لإزالة الضوضاء الغوسية من صورة سديم كارينا، وهي الصورة الأولى الملتقطة بواسطة (JWST) في 12 يوليو 2022. تم اختيار هذه المرشحات غير الخطية لتسليط الضوء على أهمية اختيار التقنية المناسبة التي يمكنها التعامل مع أكبر عدد ممكن من التفاصيل ومعالجتها والحفاظ عليها. كما أنها تعمل أيضاً على توضيح مدى التقدم الحاصل في مجال تقليل الضوضاء والتمييز بين المرشحات الكلاسيكية والمرشحات الأكثر تطوراً القادرة على التعامل مع التفاصيل الدقيقة. تتعامل المرشحات الكلاسيكية مع العناصر الصورية وجيرانها ومن ثم تقوم بإجراء العملية الإحصائية المطلوبة. بينما تأخذ المرشحات المتقدمة في الاعتبار أوجه التشابه والمسافات بين العنصر الصوري المركزي وجيرانه، وتحافظ على حواف الصورة كميزات متقدمة. وبالاعتماد على قياسات الجودة (PSNR) و(SSIM)، تمت مقارنة نتائج الترشيح، اذ أظهرت النتائج أن المرشح الثنائي يعطي أداء عالي في استعادة الصور تحت كثافات ضوضاء كاوسية مختلفة مقارنة بمرشحات تقليل الضوضاء الأخرى حيث يعطي قيم (30.65) و (0.93) لـ (PSNR) و (SSIM) على التوالي وهي أعلى من قيمة المرشح (PSNR) و (SSIM) . نتائج المرشحات.

نوع البحث: ورقة بحثية.

المصطلحات الرئيسة للبحث: إزالة الضوضاء من الصورة، استعادة الصورة، الضوضاء الغاوسية، مرشح Non Local Mean، مرشح Bilateral، المرشحات التقليدية.

(2)
(3)